

# Preparation and characterization of highly dispersed gold nanoparticles within channels of mesoporous silica

Kuei-Jung Chao\*, Ming-Hsin Cheng, You-Fu Ho, Pang-Hung Liu

*Department of Chemistry, National Tsinghua University, Hsinchu 300, Taiwan*

Received 16 November 2003; received in revised form 15 January 2004; accepted 30 March 2004

Available online 24 July 2004

## Abstract

The preparation of highly dispersed gold nanoparticles in mesoporous silica SBA-15 is monitored by in situ XAS measurement. The silanation of intrachannel surface with TPTAC can generate ion-exchange sites for anionic  $\text{Au}(\text{OH})_n\text{Cl}_{4-n}^-$  (with  $n = 0-4$ ) complex ions and help to produce uniformly dispersed gold nanoparticles in the host channels after further reduction. The average size of metal nanoparticles is dependent on the pH value of gold precursor solution.

© 2004 Elsevier B.V. All rights reserved.

**Keywords:** Gold catalyst; Mesoporous silica; XAS

## 1. Introduction

Gold is usually considered as quite inert or lack of activity in the adsorption of reactants. However, oxide supported catalysts of nanometer-size gold particles have been demonstrated recently to exhibit remarkable activity for low temperature CO oxidation, reduction of nitrogen oxides and the epoxidation of propylene, and attracted a lot of attention in catalysis technology and science [1–5]. Chemical reactivity of surface Au atoms toward the adsorption of oxygen and carbon monoxide has been investigated and considered to be derived from the quantum-size effect of gold nanoparticles, especially as their diameters fall into 2–5 nm range and the electronic interaction of metal nanoparticles with support oxides takes place [2,6].

Preparations of highly active gold catalysts were developed both by using deposition–precipitation of aqueous solution of  $\text{HAuCl}_4$  with  $\text{Na}_2\text{CO}_3$  or  $\text{NH}_4\text{OH}$  at  $\text{pH} = 6-10$  on oxide supports and by chemical vapor deposition of organometallic gold precursors onto oxide supports [3,5]. Through the interaction of anionic  $\text{Au}(\text{III})$  precursors with positively charged oxide surface, the active  $\text{TiO}_2$ ,  $\text{Fe}_2\text{O}_3$  and  $\text{Al}_2\text{O}_3$  supported gold catalysts were prepared. Their cat-

alytic activities were found to be strongly dependent on the preparation and pretreatment condition [6].

Mesoporous silica and metal oxides (such as MCM-41, -48 and SBA-15) formed by surfactant templating synthesis possess ordered channel structures and pore diameters in the range of 1.5–10 nm and large internal surface areas of 700–1000  $\text{m}^2/\text{g}$ , such features make them suitable hosts for metal nanoparticles. Direct impregnation of  $\text{AuCl}_3$  or  $\text{HAuCl}_4$  on calcined silicas to prepare supported gold catalysts was considered to be complicated due to lack of exchange or adsorption sites for anionic metal precursors on  $\text{SiO}_2$  of negatively charged surface; furthermore, high pH condition will cause the dissolution of the  $\text{SiO}_2$  support [6,7]. It was thus known to be very difficult to prepare highly dispersed and highly loaded gold nanoparticles within the channels of mesoporous silicon oxides. Preformed gold nanoparticles of 2 and 5 nm diameters were known to be encapsulated in mesoporous silicas SBA-15 and MCM-41 or -48 by growing the pore structure in the presence of metal particles with organic templates [8]. In another case, gold nanoparticles were formed by in situ reduction of aqueous chloaurate ions mixed with amine- or thiol-modified MCM-41 [9,10]; with bifunctional amine silane complexes in MCM-41 precursor solution [11]. In these methods, the removal of template molecules at low temperature is usually required to avoid the aggregation of gold nanoparticles. A novel approach was demonstrated by

\* Corresponding author. Fax: +886-3-5720964.

E-mail address: [kjchao@mx.nthu.edu.tw](mailto:kjchao@mx.nthu.edu.tw) (K.-J. Chao).

us to functionalize the template free silica surface with positive charge groups, and make the surface adsorb anionic Au complexes, the adsorbed  $\text{AuCl}_4^-$  was then reduced by  $\text{H}_2$  or  $\text{NaBH}_4$  treatment to produce active Au species to convert CO to  $\text{CO}_2$  through oxidation [4].

Detail on the preparation of Au/SBA-15 via an anion-exchange method at various pHs is discussed in this paper. Calcined mesoporous silicas possess surface silanol groups that act as anchoring points for  $(\text{CH}_3\text{O})_3\text{Si}(\text{CH}_2)_3\text{N}(\text{CH}_3)_3\text{Cl}$  (TPTAC) and give  $\text{SBA-15-PTA}^+\text{Cl}^-$ ,  $\text{Cl}^-$  ions have been exchanged with anionic  $\text{Au}(\text{OH})_n\text{Cl}_{4-n}^-$  (with  $n = 0-4$ ) complex ions at  $\text{pH} = 2-8$  in an aqueous  $\text{HAuCl}_4$  solution for the preparation of Au/SBA-15 with Au wt.% of 4–9. The results of powder X-ray diffraction (PXRD), transmission electron microscopy (TEM), gravimetric thermal analysis,  $\text{N}_2$ -porosimetry, X-ray absorption (XAS) including EXAFS and XANES characterizations are presented. It indicates that the pH value of  $\text{HAuCl}_4$  aqueous solution affects not only the nature of the chloroaurate species and gold loading but also the size and location of gold nanoparticles on SBA-15 silica.

## 2. Experimental

### 2.1. Catalysts preparation

Siliceous SBA-15 was synthesized using  $(\text{EO})_{20}\cdot(\text{PO})_{70}\cdot(\text{EO})_{20}$  triblock copolymer (P123) as template following the literature procedure [12]. The mesoporous silica was calcined at  $540^\circ\text{C}$  to remove the organic templates and accompanied this with also the partial loss of surface hydroxyl groups. Prior to surface functionalization, a 0.5 g aliquot of calcined SBA-15 was rehydrated with water vapor at  $\sim 27,000\text{ Pa}$  and  $100^\circ\text{C}$  for 30 min, and it was then suspended in a solution of 25 ml toluene and 8 ml TPTAC (50 wt.% in methanol, Gelest). The mixture was stirred at room temperature for 12 h and refluxed at  $70^\circ\text{C}$  for 24 h, and then the solid part was washed thoroughly with ethanol ( $\sim 300\text{ ml}$ ) and dried at  $60^\circ\text{C}$  for 8 h to give  $\text{SBA-15-PTA}^+\text{Cl}^-$ .

For gold-loading process, 0.4 g of the dried  $\text{SBA-15-PTA}^+\text{Cl}^-$  was suspended in 6 ml 0.1 M  $\text{HAuCl}_4$  (Showa) aqueous solution at  $\text{pH} \cong 2$ . After filtration, the retaining solid was washed with 10 ml ethanol and drying at  $45^\circ\text{C}$  for 8 h, the resulting yellowish solid was designated as an as-prepared sample and it was further reduced in a flow of 10%  $\text{H}_2$  and 90% Ar at  $200^\circ\text{C}$  for 4 h (with the flow rate of 40 ml/min and the ramping rate of  $1^\circ\text{C}/\text{min}$  from room temperature to  $200^\circ\text{C}$ ) to give Au2/SBA-15(r).

A chloroaurate complex solution of pH 5 was prepared by adding 17 ml 0.1 M NaOH solution to 100 ml 0.005 M aqueous  $\text{HAuCl}_4$  solution dropwise over 1 day. A 0.5 g aliquot of dried  $\text{SBA-15-PTA}^+\text{Cl}^-$  was suspended in the chloroaurate solution of pH 5 and stirred for 12 h. The solid was precipitated by centrifuging, the supernatant liquid was

discarded, and then washed with de-ionized water three times. The resulting solid was dried at  $45^\circ\text{C}$  for 8 h, and gave a light yellow Au5/SBA-15-C and it was further reduced at  $150^\circ\text{C}$  for 4 h to give Au5/SBA-15-C(r). In another case, the solid was filtered and washed with de-ionized water until it was free of  $\text{Cl}^-$  ions as tested by adding  $\text{AgNO}_3$  solution. This sample was then dried at  $45^\circ\text{C}$ . The reduction process was performed in the flow of 10%  $\text{H}_2$  and 90% Ar at  $300^\circ\text{C}$  for 2 h to give Au5/SBA-15-F(r).

Another 0.5 g aliquot of  $\text{SBA-15-PTA}^+\text{Cl}^-$  was suspended in a chloroaurate aqueous solution at pH 8, which was pre-adjusted and maintained at pH 8 by adding dropwise 13 ml 0.2 M NaOH and 4 ml de-ionized water to 100 ml 0.005 M  $\text{HAuCl}_4$  solution over 1 day. After filtration, washing, drying and reduction at  $300^\circ\text{C}$ , the resulting sample was designated as Au8/SBA-15(r).

### 2.2. Characterization

The gold-loaded SBA-15 samples were digested in mixed acid and their compositions were obtained by ICP-AES analysis using a Jarrell-Ash-ICAP 9000 device. In situ XAS investigation was done in transmission mode on the wiggler beamline BL17C of the National Synchrotron Radiation Research Center (NSRRC), Taiwan, with storage ring energy of 1.5 GeV and a beam current between 100 and 200 mA. Prior to the XAS measurement, the as-prepared sample was mounted in an in situ cell and dried at  $80^\circ\text{C}$  for 12 h under the flow of He, then cooled to room temperature. The reduced sample was obtained by heating the as-prepared sample to 150, 200 or  $300^\circ\text{C}$  at a heating rate of  $1^\circ\text{C}/\text{min}$  under the flow (40 ml/min) of 10%  $\text{H}_2$  in Ar, and the sample was maintained at 150, 200 or  $300^\circ\text{C}$  for 2 h under the flow of  $\text{H}_2/\text{Ar} = 1/9$  and cooled to room temperature under He flow. The XAS spectra of as-prepared and reduced samples were collected under the He flow. PXRD patterns were collected on the beamline BL17A of NSRRC. TEM and EDX were carried out on a JEOL JEM-2010 electron microscope equipped with an Oxford EDX analysis system. Samples were embedded in resin and ultramicrotomed into slices with thickness at  $\sim 50\text{ nm}$  for TEM and EDX investigations. The pore diameter, pore volume, and surface area of the samples were derived from the nitrogen sorption isotherms at 77 K and Barrett-Joyner-Halenda (BJH) method using a Micromeritics ASAP 2010 system.

## 3. Results and discussion

### 3.1. Au complexes in as-prepared Au/SBA-15s

Gold ions in chloride solution were considered predominately in Au(III) rather than Au(I) at temperature below  $150-200^\circ\text{C}$  [13]. An aqueous solution of  $\text{HAuCl}_4$  at pH 2 gives  $\text{AuCl}_4^-$  as major anionic species.  $\text{AuCl}_4^-$  ions undergo hydrolysis and react with NaOH to give soluble

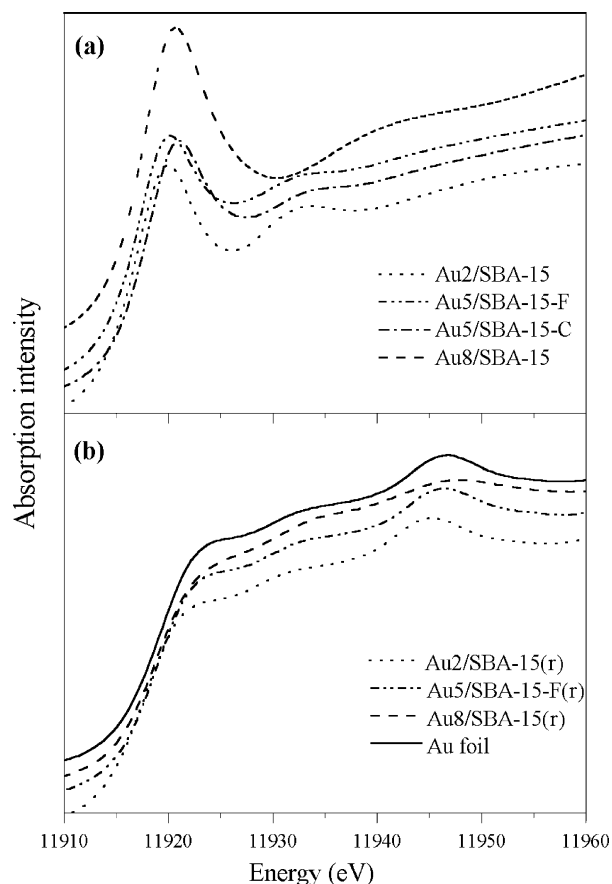


Fig. 1. Au L<sub>III</sub>-edge XANES spectra of (a) synthesized samples and (b) reduced samples.

chloroaurate species, which can, in turn, be used as precursors for mesoporous silica supports. The forms of gold species in the as-prepared and reduced composites were monitored by in situ XAS measurement.

The XAS spectra were measured from 200 below to 1200 eV above the Au L<sub>III</sub>-edge (11,919 eV) and standard Au foil was used as a reference for energy calibration as shown in Fig. 1. Position of the first inflection point of an

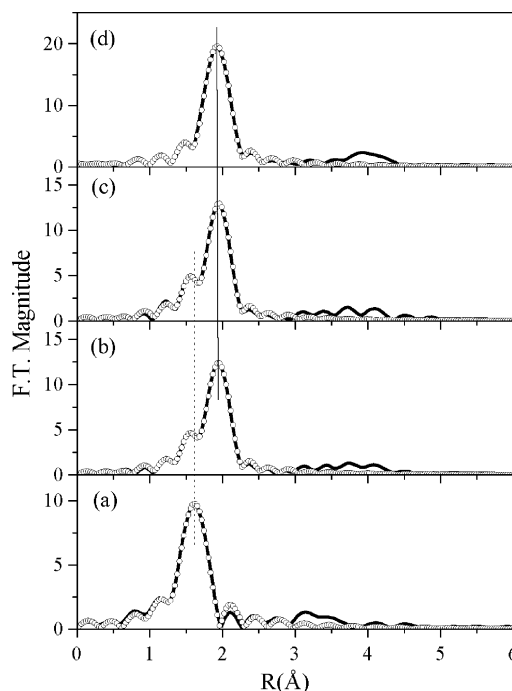


Fig. 2. Fourier transforms of Au L<sub>III</sub>-edge  $k^3$ -weighted EXAFS data for as-synthesized Au8/SBA-15 (a), Au5/SBA-15-F (b), Au5/SBA-15-C (c) and Au2/SBA-15 (d). Solid lines and open circles are the experimental and the fitted results, respectively. Note that the phase shifts were not corrected.

absorption near-edge curve (threshold energy) was found to be sensitive to oxidation state of a metal, and  $\sim 2$  eV lower for Au complexes in as-prepared samples than that for reduced samples and Au foil (Fig. 1). This clearly confirms the Au(III) form in adsorbed chloroaurate complexes and its further reduction to Au (0) after H<sub>2</sub>-treatment. The resonance feature located at 15–49 eV past the edge corresponds to the local structure around the Au atom; the profile of as-prepared Au8/SBA-15 is different from that of other as-prepared Au/SBA-15s. Fourier transform (FT) profiles of  $k^3$ -weighted Au L<sub>III</sub>-edge EXAFS and curve fitting results are shown in Fig. 2 and Table 1. The EXAFS of

Table 1

Au L<sub>III</sub>-edge EXAFS results of as-synthesized and reduced Au/SBA-15 samples and estimated sizes of gold nanoparticles

Sample	Thermal treatment	Au L <sub>III</sub> -edge					Particle size (diameter, nm)	
		Shell	CN	$R$ (Å)	$\sigma^2$ ( $\times 10^{-3}$ Å <sup>2</sup> )	$r$ -Factor	EXAFS <sup>a</sup>	TEM
Au2/SBA-15	–	Au–Cl	4.0	2.30	2.4	0.0022	–	–
Au2/SBA-15(r)	200 °C	Au–Au	11.7	2.87	8.2	0.0043	>10	>30
Au5/SBA-15-C	–	Au–Cl	2.4	2.30	2.3	0.0011	–	–
		Au–O	1.2	2.00	4.9			
Au5/SBA-15-C(r)	150 °C	Au–Au	10.1	2.85	8.9	0.0291	$\sim 3$	5
Au5/SBA-15-F	–	Au–Cl	2.3	2.30	2.4	0.0015	–	–
		Au–O	1.1	2.00	5.2			
Au5/SBA-15-F(r)	300 °C	Au–Au	10.9	2.87	8.3	0.0019	$\sim 5$	–
Au8/SBA-15	–	Au–O	3.4	1.99	2.6	0.0098	–	–
Au8/SBA-15(r)	300 °C	Au–Au	7.3	2.78	11.6	0.0086	$\sim 1$	$\sim 1$
		Au–Au	12.0	2.87	8.1			
Au-foil	–	Au–Au	12.0	2.87	8.1	0.0076	–	–

<sup>a</sup> The sizes were estimated from a gold spherical model with face-centered cubic structure.

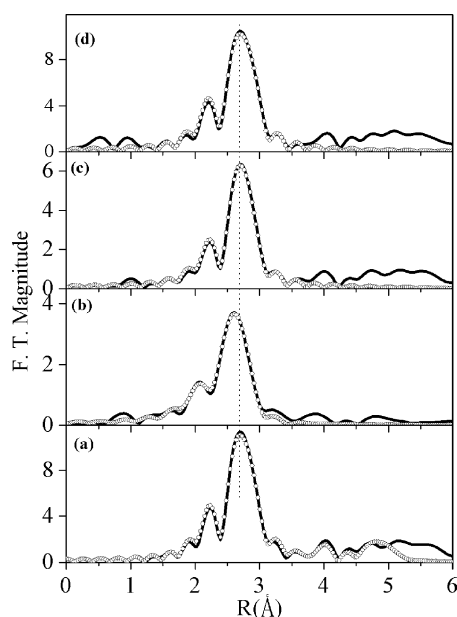


Fig. 3. Fourier transforms of Au L<sub>III</sub>-edge  $k^3$ -weighted EXAFS data for Au foil (a), and reduced samples: Au8/SBA-15(r) (b), Au5/SBA-15-F(r) (c) and Au2/SBA-15(r) (d). Solid lines and open circles are the experimental and the fitted results, respectively. Note that the phase shifts were not corrected.

as-prepared Au2/SBA-15 shows the presence of 4.0 Au–Cl bonds with a bond length of 2.3 Å, close to that of  $\text{AuCl}_4^-$  supported on SBA-15; hence, as expected  $\text{AuCl}_3(\text{OH})^-$  and  $\text{AuCl}_2(\text{OH})_2^-$  are present on as-prepared Au5/SBA-15 and  $\text{Au}(\text{OH})_3$  or  $\text{AuCl}(\text{OH})_3^-$  and  $\text{Au}(\text{OH})_4^-$  are present on as-prepared Au8/SBA-15, and the forms of adsorbed gold species on mesoporous silica are similar to the chloroaurate complexes in aqueous solution  $\text{HAuCl}_4$  at various pH values, as detected previously using Raman spectroscopy [13,14]. Unexpectedly, Au species were found to be mainly in the form of Au–O bonding for  $\text{AuCl}_3$  onto  $\gamma\text{-Al}_2\text{O}_3$  under pHs from 4 to 9 and as-prepared by the deposition method [15];  $\text{Au}(\text{OH})_3$  precipitate was considered to be the dominating species in the equilibrated impregnation-solution with a pH range from 5 to 9 [16].

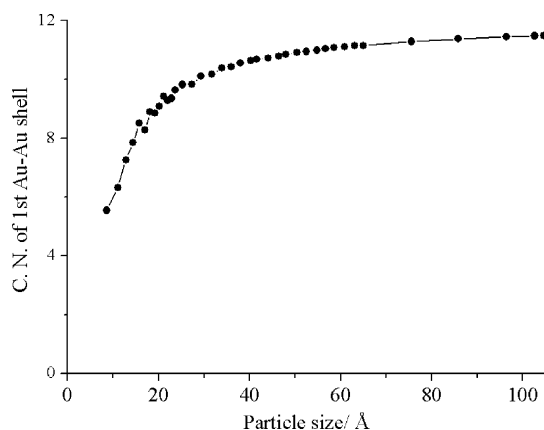


Fig. 4. The calculated relation between first shell coordination number and particle size of Au nanoparticles.

The ion-exchange behavior of functionalized mesoporous silica was found to depend upon the nature of anionic complexes in solution. The resulting Au loading of Au2/SBA-15(r) is 9 wt.% and those of Au5/SBA-15-F(r), Au5/SBA-15-C(r) and Au8/SBA-15(r) are 4–6 wt.%.

### 3.2. Reduction and decomposition of adsorbed chloroaurate complexes

After reduction at 150, 200 or 300 °C, EXAFS profiles of Au/SBA-15(r) samples mainly consist of a first-shell

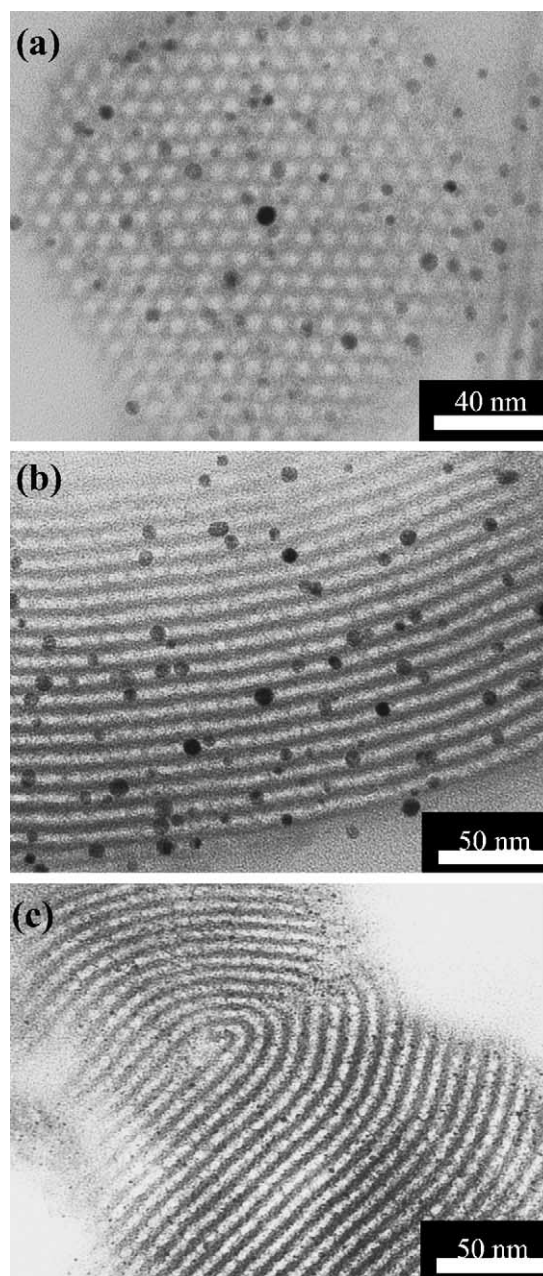


Fig. 5. TEM images of Au5/SBA-15(r) along the [100] (a) and [110] (b) zone axes of SBA-15, and Au8/SBA-15(r) along the [110] zone axis of SBA-15 (c).



Au–Au peak (Fig. 3). The presence of an Au–Au distance of 2.85–2.87 Å together with coordination numbers (CN) of 10 and 12 in Au5/SBA-15(r) and Au2/SBA-15(r), respectively, indicates the generation of 5 nm and larger Au particles. On Au8/SBA-15(r), the Au–Au bond distance is of 2.78 Å, accompanied by CN = 7.3 as indicated in Table 1. The CN value is lower than the ideal value (7.85) for a cuboctahedral cluster of 55 atoms with diameter = 1.2 nm but higher than that (6.5) for ligand-stabilized compound Au<sub>55</sub>(PPh<sub>3</sub>)<sub>12</sub>Cl<sub>6</sub> with diameter = 1.8 nm [17,18]. The contraction of Au–Au distance has also been reported in Au<sub>55</sub>(PPh<sub>3</sub>)<sub>12</sub>Cl<sub>6</sub> species.

Following Jeutys's calculation [19], Au cluster models were generated using the "ATOMS" program by gradually increasing the "radial size of the cluster" parameter, and Au clusters with different diameters were built based on the bulk f.c.c. structure. These built clusters were either in cuboctahedral shape (e.g. 13, 15 and 147-atom clusters etc.) or in other less regular shapes. The average coordination number of an atom in a cluster, the sum of number of first-shell neighbors of every atom in the cluster divided by the number of atoms in the cluster, varies with the value of cluster size as shown in Fig. 4. It indicates that particle sizes of values less than 3 nm can be easily estimated from corresponding coordination numbers and usually can not be detected by PXRD.

TEM images of Fig. 5a and b clearly show uniform and highly dispersed Au nanoparticles with diameter  $\cong$  5 nm in the hexagonal packed channels of SBA-15 on Au5/SBA-15(r). In Au8/SBA-15(r), the Au particles are quite small ( $\sim$ 1 nm) and are exclusively stayed inside the channels of the host SBA-15, and this is in good agreement with the results of in situ EXAFS and PXRD analyses.

The SBA-15 still exhibits a two-dimensional mesostructure of P6mm symmetry after reduction as shown in its TEM images (Fig. 5). The average wall thickness of the mesochannels ( $t = 2d_{100}/3^{1/2} - D = 5.6$  nm) was estimated from PXRD pattern of calcined SBA-15 with  $d_{100}$  spacing of ca. 9.2 nm and N<sub>2</sub> adsorption of pore size ( $D$ ) of ca. 5 nm. Both the calcined and dehydrated mesoporous silica SBA-15 and the dehydrated Au/SBA-15(r) exhibit similar N<sub>2</sub> adsorption–desorption isotherms with narrow hysteresis loops at 77 K. It reveals that the metal nanoparticles disperse through the entire channels, instead of being in agglomerate

form. The presence of decreased surface area and pore volume may be an indication of loading of the metal nanoparticles within the pores.

#### 4. Conclusion

In this study, the XAS investigation monitored the hydrolysis of AuCl<sub>4</sub><sup>−</sup> to AuCl<sub>x</sub>(OH)<sub>4−x</sub><sup>−</sup>, and the ion-exchange of AuCl<sub>x</sub>(OH)<sub>4−x</sub><sup>−</sup> with SBA-15-PTA<sup>+</sup>Cl<sup>−</sup>. The cationic groups on intrachannel surface have been found to act as binding sites for the chloroaurate anions and the intrameso-channel voids provide the confined space for the gold nanoparticles.

#### References

- [1] T.M. Salama, R. Ohmishi, T. Shido, M. Ichikawa, J. Catal. 162 (1996) 169.
- [2] T. Hayashi, K. Tanaka, M. Haruta, J. Catal. 178 (1998) 566.
- [3] G.C. Bond, Catal. Today 72 (2002) 5.
- [4] C.M. Yang, M. Kalwei, F. Schüth, K.J. Chao, Appl. Catal. A, in press;  
C.M. Yang, P.H. Liu, Y.F. Ho, C.Y. Chiu, K.J. Chao, Chem. Mater. 15 (2003) 275.
- [5] M. Haruta, M. Daté, Appl. Catal. A 222 (2001) 427.
- [6] A. Wolf, F. Schüth, Appl. Catal. A 226 (2002) 1.
- [7] P.A. Sermon, J. Sivalingam, Colloids Surf. 63 (1992) 59.
- [8] Z. Kónya, V.F. Puentes, I. Kiricsi, J. Zhu, J.W. Ager, M.K. Ko, H. Frei, P. Alivisatos, G.A. Somorjai, Chem. Mater. 15 (2003) 1242.
- [9] P. Mukherjee, M. Sastry, R. Kumar, Physchemcomm (2000) 4.
- [10] Y. Guari, C. Thieuleux, A. Mehdi, C. Reyé, R. J.P. Corriu, S. Gomez-Gallardo, K. Philippot, B. Chaudret, R. Dutartre, Chem. Commun. (2001) 1374.
- [11] H.G. Zhu, B. Lee, S. Dai, S.H. Overbury, Langmuir 19 (2003) 3974.
- [12] D.Y. Zhao, J.L. Feng, Q.S. Huo, N. Melosh, G.H. Fredrickson, B.F. Chmelka, G.D. Stucky, Science 279 (1998) 548.
- [13] P.J. Murphy, M.S. LaGrange, Geochim. Cosmochim. Acta 62 (1998) 3515.
- [14] P. Pan, S.A. Wood, Geochim. Cosmochim. Acta 55 (1991) 2365.
- [15] C.H. Lin, S.H. Hsu, M.Y. Lee, S.D. Lin, J. Catal. 209 (2002) 62.
- [16] C.K. Chang, Y.J. Chen, C.T. Yeh, Appl. Catal. A 174 (1998) 13.
- [17] P. Scardi, P.L. Antonucci, J. Mater. Res. 8 (1993) 1829.
- [18] R.E. Benfield, D. Grandjean, M. Kröll, R. Pugin, T. Sawitowski, G. Schmid, J. Phys. Chem. B 105 (2001) 1961.
- [19] A. Jeutys, Phys. Chem. Chem. Phys. 1 (1999) 4059.